A novel approach to assess post-yield energy dissipation of bone in tension

Xiaodu Wang[*] and **Jeffry S. Nyman**
Department of Mechanical Engineering, University of Texas at San Antonio, 6900 North Loop 1604 West, San Antonio, TX 78249, USA

Abstract

In this study, we proposed a novel approach to assess the energy dissipation during the post-yield deformation of bone. Based on the stress–strain behavior in an incremental and cyclic loading–unloading–reloading scheme in uniaxial tension, we partitioned the post-yield energy dissipation of bone into three distinct pathways: released elastic strain energy (U_{er}); irreversible energy (U_i); and hysteresis energy (U_h). Among them, U_{er} depends on the stiffness loss, U_i is the energy permanently consumed, and U_h reflects changes in the viscoelastic behavior of bone in the process of post-yield deformation. As an example, bone specimens from human cadaveric femurs of middle-aged and elderly donors were tested using this approach. The results of this study indicate that there exist age-related differences in post-yield energy dissipation and modulus degradation. These results implicate that this novel approach could detect the age-related differences in energy dissipation of bone and may aid in understanding the underlying mechanisms of such changes.

Keywords

Bone; Toughness; Energy dissipation; Tension; Microdamage

1. Introduction

Age-related degradation in toughness makes bone more susceptible to fracture (Burstein et al., 1976). The observed decrease in bone toughness with age likely depends on the age-related changes in the post-yield behavior of bone (McCalden et al., 1993). However, underlying mechanisms of post-energy dissipation in bone is still not clear. Previous studies have reported that microdamage accumulation (including both linear microcrack and diffuse damage) may be major mechanisms in energy dissipation during the post-yield deformation of bone (Courtney et al., 1996; Jepsen and Davy, 1997; Kotha and Guzelsu, 2003; Martin et al., 1997; Zioupos and Currey, 1998). In addition, age- or disease-related changes in the collagen network may also contribute to the reduced bone toughness (Jepsen et al., 1996; Wang et al., 2002; Zioupos et al., 1999), indicating the involvement of collagen in post-yield energy dissipation. These previous studies implicate that the post-yield energy dissipation in bone may be associated with several pathways. Thus, partitioning the energy dissipation during the post-yield deformation of bone may help elucidate the underlying mechanism of age-related bone fractures. To address this issue, we proposed a novel methodology to assess the energy dissipation pathways during the post-yield deformation of bone.

[*]Corresponding author. Tel.: +1210 458 5565; fax: +1210 458 6504. *E-mail addresses:* xwang@utsa.edu, xiaodu.wang@utsa.edu (X. Wang).

2. Materials and methods

2.1. Loading procedure

Using a load–unload–reload scheme as shown in Fig. 1, we proposed to partition post-yield energy into three components during the cycle: the released elastic strain energy (i.e., the area enclosed in HEF or U_{er}), hysteresis energy (i.e., the area enclosed in the unloading and reloading loop or U_h), and the irreversible energy (i.e., the area enclosed in ABCG or U_i). The released elastic strain energy is mainly due to the modulus loss (Fondrk et al., 1999a,b). The hysteresis energy reflects the viscoelastic behavior of bone in the process of load bearing (Doubal et al., 2004). Finally, the irreversible energy dissipation (U_i) involves at least two possible pathways: formation of new cracks (U_{er}) and permanent deformation (U_p) in the tissue (Fondrk et al., 1999a,b). The underlying mechanisms involved in these pathways are still unclear. However, previous studies have shown that microdamage accumulation is related to the loss of the stiffness of bone (Burr et al., 1998). In addition, the integrity of the collagen network significantly affects the toughness (Wang et al., 2001) and the post-yield stress–strain behavior of bone (Wright et al., 1981). Moreover, A microstructural barrier (e.g., cement lines), which slows the growth of cracks during fatigue loading, may also affect post-yield behavior of bone (O'Brien et al., 2003).

To distinguish between these different pathways of energy dissipation, a progressive load–unload–reload scheme in uniaxial tension was implemented as shown in Fig. 2. An incremental displacement of 0.05 mm was imposed on the specimen for each cycle (Table 1). Strain was estimated as the change of the crosshead displacement per 10 mm gage region. In each cycle, the specimen was first loaded under displacement control to the next displacement level at a rate of 5 mm/min; then held steady for 60 s for stress relaxation (from point C to H as shown in Fig. 1). Thereafter, the specimen was unloaded in load control to zero force, and held for 60 s for strain relaxation (from point F to G as shown in Fig. 1), and then reloaded again in displacement control to the next strain level. This process was repeated until failure. All specimens that did not fail at the sixth cycle were loaded to failure without further cycles. The bone specimens were kept moist by wrapping them with gauze soaked with physiological saline.

In the incremental loading scheme (Fig. 2), the total irreversible energy (U_i) absorbed by the specimen at the previous and present cycles is actually the result of cumulative deformation of each loading cycle, and can be simply calculated as the summation of each U_i of all previous and present loading cycles. On the other hand, U_{er} and U_h measured at each cycle already represent the cumulative effect. The permanent strain energy portion (U_p) of the total irreversible energy (U_i) was estimated as $U_i - U_{er}$. Also, we calculated the toughness ($U_T = U_i + U_{er} + U_h + U_{e0} + U_L$) and the ultimate strength (σ_{max}) for each bone specimen as shown in Fig. 2. To investigate the contribution of each post-yield energy term to the total energy dissipation, we used the ratio of each energy term (i.e., U_p, U_{er}, and U_h) to the overall energy capacity ($U_S = U_i + U_{er} + U_h + U_{e0}$ in Fig. 2) at the final cycle.

The elastic modulus after yielding was calculated as the slope of line HG (presumably between two equilibrium points) in order to avoid the influence of viscoelasticity (hysteresis). Moreover, the modulus degradation at the each cycle was estimated as ($1 - E_f/E_0$), where E_0 is the initial elastic modulus and E_f is the elastic modulus at the cycle.

2.2. Bone specimen preparation

Eighteen tensile specimens were prepared each from 18 male cadaveric femurs that were collected from Texas Willed Body Program and National Disease Research Exchange. The specimens were evenly divided into two age groups ($n = 9$): middle-aged (49–59 years) and

elderly (69–87 years). The 'dog bone' specimens (10 mm × 5 mm grip regions and a 10 mm × 2 mm gage region) were prepared longitudinally from the middiaphysis of each femur using a diamond saw and a CNC machine (ProLIGHT 1000, Light Machines, Manchester, NH).

2.3. Statistical analysis

Student's t-tests (one tail) were performed to examine the age-related effects on the post-yield energy dissipation and other aforementioned properties of bone. Significant differences were considered only if p-value was less than 0.05.

3. Results

Table 1 shows the number of survival specimens (no failure) at each incremental loading cycle. It was observed that after 2.0% strain the number of survival specimens in the middle-aged group was consistently higher than that in the elderly one. Also, it was observed that no difference in U_p exists at cycle 3 (Fig. 3), but at the final cycle between the age groups (Table 2). As shown in Table 2, U_p, U_{er}, σ_u, and modulus degradation of bone deceased significantly with age ($p<0:05$). U_T and U_h of bone did indicate a trend of decrease with age although their p-values are little higher than 0.05 ($p<0:06$). It is noteworthy that the age-related differences were very similar in all energy dissipation terms (about 30–35%), while the differences in strength and modulus degradation were somewhat smaller (around 13–15%).

Furthermore, the relative contribution of the post-yield energy terms to the energy capacity of bone did not show significant differences between the age groups in the early cycles (Fig. 3), with permanent strain energy (U_p) having the greatest contribution to energy dissipation. However, significant age-related differences were observed in the total energy dissipation of bone (Table 3). Lastly, with an increase in post-yield deformation, age first affected U_{er} and then U_p (Table 2 and Fig. 3).

4. Discussion

The results of this study indicate that the proposed experimental approach may be of use in distinguishing the different pathways of energy dissipation in the post-yield deformation of bone. Conventional approaches, such as fracture toughness testing, give the bulk properties, but cannot distinguish between contributions of bone constituents to bone toughness. The advantage of the present approach is that it may provide more specific information to help understand changes in the bone constituents as a function of aging or other bone diseases.

There are some limitations to the current approach. First, this approach has only been tested in uniaxial tension. While energy dissipation during tensile yielding is informative, failure of bone certainly occurs in the other modes of loading. Diagnostic tests investigating the effect of damage by overload on mechanical properties of cortical bone indicated similar post-yield behavior in torsion (Jepsen and Davy, 1997) and compression (Morgan et al., 2005), but failure appears to occur at lower strain levels. Second, since the bone specimens did not break exactly at prescribed strain levels, we used the post-yield energy dissipation at the last complete cycle as an approximation of those terms at failure. In fact, such errors could be limited by reducing the incremental loading displacement.

There is one intriguing observation in the experimental results obtained using the proposed approach: That is, age-related decreases are more significant in the post-yield energy dissipation than in the modulus degradation (stiffness loss) of bone, suggesting that aging has more effects on the post-yield energy dissipation than on the stiffness loss of bone.

References

Burr DB, Turner CH, Naick P, Forwood MR, Ambrosius W, Hasan MS, Pidaparti R. Does microdamage accumulation affect the mechanical properties of bone? Journal of Biomechanics 1998;31:337–345. [PubMed: 9672087]

Burstein AH, Reilly DT, Martens M. Aging of bone tissue: mechanical properties. Journal of Bone and Joint Surgery—American 1976;58:82–86.

Courtney AC, Hayes WC, Gibson LJ. Age-related differences in post-yield damage in human cortical bone. Experiment and model. Journal of Biomechanics 1996;29:1463–1471. [PubMed: 8894927]

Doubal S, Klemera P, Semeckây V, Lamka J, Kucharovâa M. Non-linear mechanical behavior of visco-elastic biological structures—measurements and models. Acta medica (Hradec Krâalovâe)/Universitas Carolina, Facultas Medica Hradec Krâalovâe 2004;47:297–300.

Fondrk MT, Bahniuk EH, Davy DT. A damage model for nonlinear tensile behavior of cortical bone. Journal of Biomechanical Engineering 1999a;121:533–541. [PubMed: 10529922]

Fondrk MT, Bahniuk EH, Davy DT. Inelastic strain accumulation in cortical bone during rapid transient tensile loading. Journal of Biomechanical Engineering 1999b;121:616–621. [PubMed: 10633262]

Jepsen KJ, Davy DT. Comparison of damage accumulation measures in human cortical bone. Journal of Biomechanics 1997;30:891–894. [PubMed: 9302611]

Jepsen KJ, Goldstein SA, Kuhn JL, Schaffler MB, Bonadio J. Type-I collagen mutation compromises the post-yield behavior of Mov13 long bone. Journal of Orthopaedic Research 1996;14:493–499. [PubMed: 8676263]

Kotha SP, Guzelsu N. Tensile damage and its effects on cortical bone. Journal of Biomechanics 2003;36:1683–1689. [PubMed: 14522210]

Martin RB, Gibson VA, Stover SM, Gibeling JC, Griffin LV. Residual strength of equine bone is not reduced by intense fatigue loading: implications for stress fracture. Journal of Biomechanics 1997;30:109–114. [PubMed: 9001930]

McCalden RW, McGeough JA, Barker MB, Court-Brown CM. Age-related changes in the tensile properties of cortical bone. The relative importance of changes in porosity, mineralization, and microstructure. Journal of Bone and Joint Surgery—American 1993;75:1193–1205.

Morgan EF, Lee JJ, Keaveny TM. Sensitivity of multiple damage parameters to compressive overload in cortical bone. Journal of Biomechanical Engineering 2005;127:557–562. [PubMed: 16121524]

O'Brien FJ, Taylor D, Lee TC. Microcrack accumulation at different intervals during fatigue testing of compact bone. Journal of Biomechanics 2003;36:973–980. [PubMed: 12757806]

Wang X, Bank RA, TeKoppele JM, Agrawal CM. The role of collagen in determining bone mechanical properties. Journal of Orthopaedic Research 2001;19:1021–1026. [PubMed: 11781000]

Wang X, Shen X, Li X, Agrawal CM. Age-related changes in the collagen network and toughness of bone. Bone 2002;31:1–7. [PubMed: 12110404]

Wright TM, Vosburgh F, Burstein AH. Permanent deformation of compact bone monitored by acoustic emission. Journal of Biomechanics 1981;14:405–409. [PubMed: 7263733]

Zioupos P, Currey JD. Changes in the stiffness, strength, and toughness of human cortical bone with age. Bone 1998;22:57–66. [PubMed: 9437514]

Zioupos P, Currey JD, Hamer AJ. The role of collagen in the declining mechanical properties of aging human cortical bone. Journal Of Biomedical Materials Research 1999;45:108–116. [PubMed: 10397964]
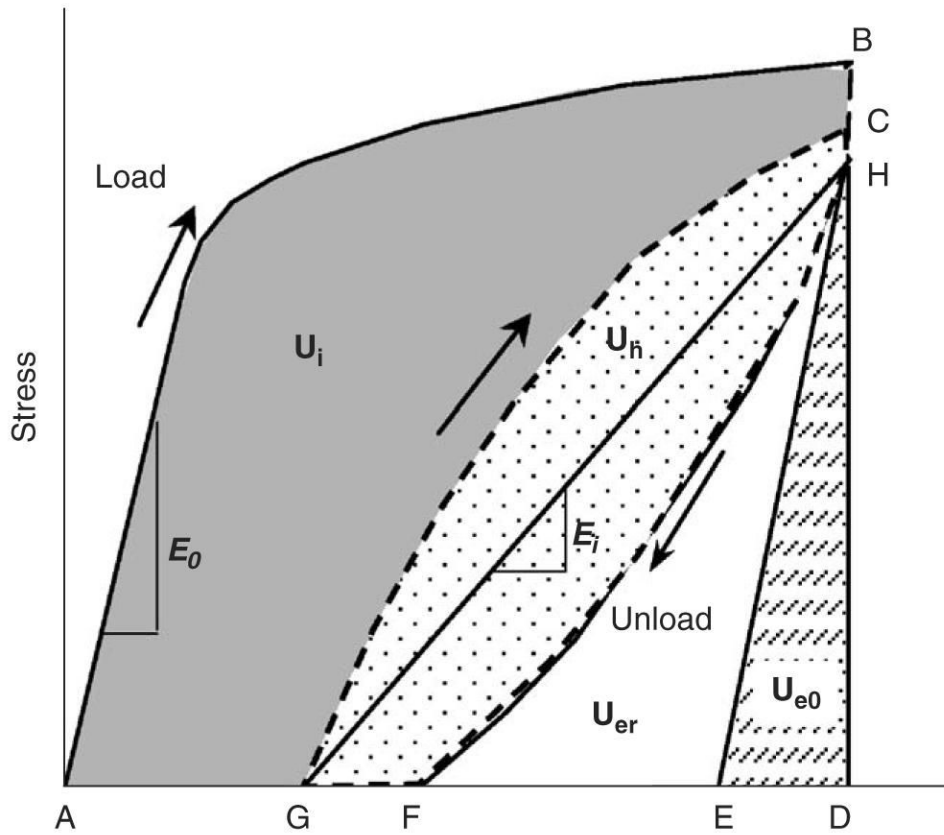
Fig. 1.
Partitioning the energy capacity of bone: nominal elastic strain energy (U_{e0}) depending on the initial elastic modulus (E_0); released elastic strain energy (U_{er}) relating to modulus degradation; hysteresis energy (U_h) reflecting the viscoelastic nature of bone; and irreversible energy (U_i) dissipation, which reflects the free surface energy released by microdamage formation (U_{er}) and the permanent strain energy (U_p).
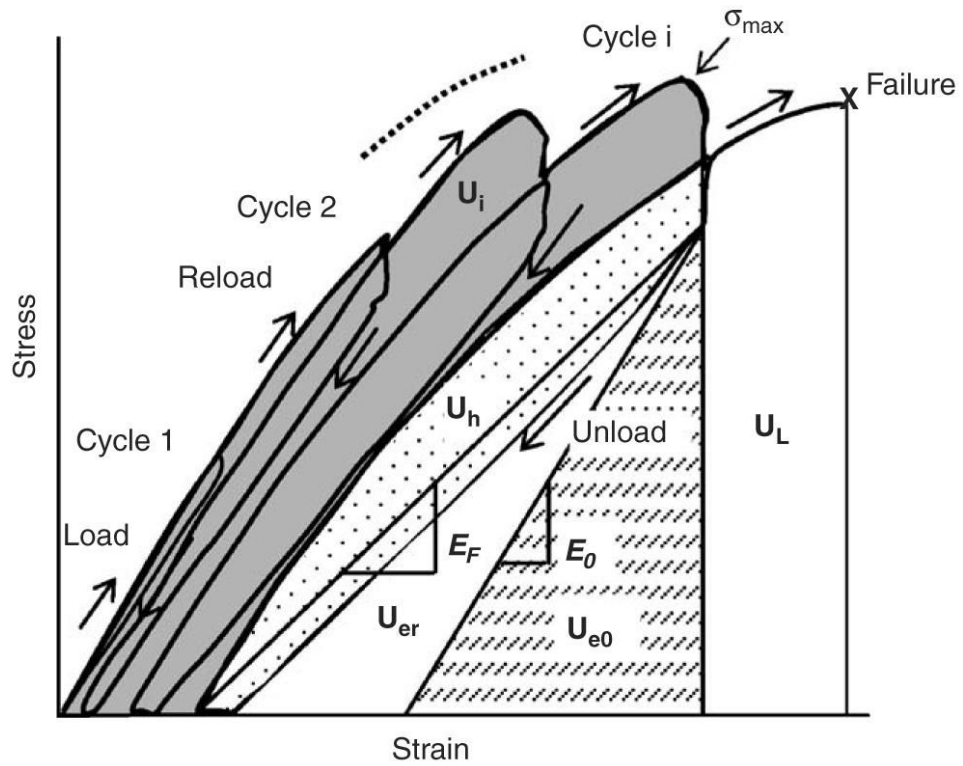
Fig. 2.
The cyclic loading scheme was used with a displacement increment of 0.05 mm (approximately 0.5% strain) at each successive cycle. The energy terms could be calculated for each cycle. In this example, failure occurred after the fourth cycle, but before the fifth cycle. U_I is estimated as the gray shaded area for the last cycle. The toughness ($U_T = U_I + U_{er} + U_h + U_{e0} + U_L$) was calculated as a summation of all energy terms including U_L.
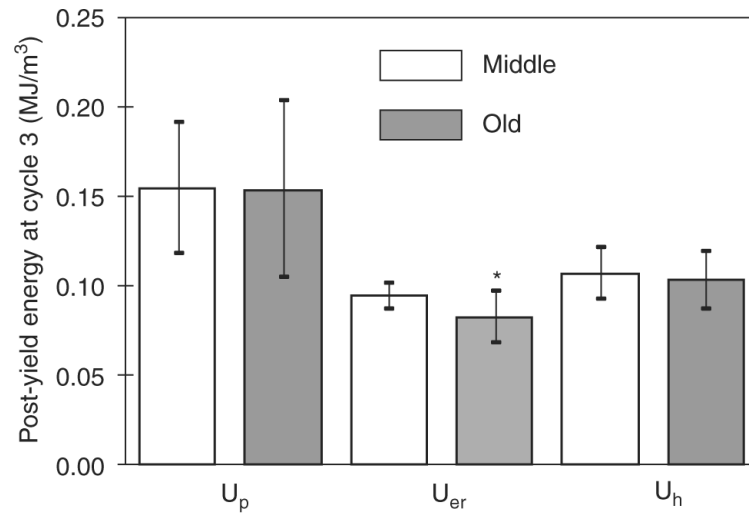
Fig. 3.
Post-yield energy dissipation at the early stage of post-yield deformation (at cycle 3) does show significant age-related effects in energy dissipation except for the released elastic strain energy ($p = 0.027$). *indicates significant difference between the two age groups ($p<0.05$).

Table 1

Number of survival specimens (no failure) at incremental displacement is greater in middle-aged bone as indicated by the greater number of surviving specimens at greater displacement

Cycle (*i*th)	Displacement (mm)	Estimated strain	Middle-aged	Elderly
1	0.05	0.005	9	9
2	0.10	0.010	9	9
3	0.15	0.015	9	9
4	0.20	0.020	9	6
5	0.25	0.025	7	4
6	0.30	0.030	4	2
Final	Till failure	>0.030	3	2

Table 2

Summary of experimental results obtained at the last cycle prior to failure ($N = 9$)

Properties	Middle-aged	Elderly	*p*-value
Plastic strain energy U_p (MJ/m^3)	0.674±0.257	0.403±0.230	0.016
Released elastic strain energy U_{er} (MJ/m^3)	0.298±0.099	0.199±0.126	0.042
Hysteresis energy U_h (MJ/m^3)	0.320±0.092	0.229±0.134	0.058
Toughness U_T (MJ/m^3)	2.48±0.975	1.740±0.856	0.054
Strength σ_{max} (MPa)	88.1±11.4	75.6±13.0	0.023
Final modulus degradation ($1-E_F/E_0$)	0.48±0.05	0.41±0.09	0.047

Table 3

Relative contribution of each final post-yield energy term to the energy capacity of middle-aged and elderly bone ($N = 9$)

Properties	U_p/U_S (%)	U_{er}/U_S (%)	U_h/U_S (%)
Middle-aged	34.4±5.3	15.4±1.5	16.8±1.1
Elderly	28.7±7.3[a]	13.5±2.3	16.5±1.9

[a]Significantly less than the middle-aged group (p-value<0.05).